Tr. J. of Chemistry
21 (1997) , 35 - 41.

Dissociation Dynamics of Small Carbon Clusters*

Ersin YURTSEVER
Koç University, Chemistry Department,
İstinye, 80860 İstanbul-TURKEY
Nuran ELMACI
Middle East Technical University, Chemistry Department,
Ankara-TURKEY

Received 10.1.1997

The dissociation dynamics of small carbon clusters is studied by classical trajectory analysis. A large number of initial conditions are chosen to analyze the effects of the energy, angular momentum and the initial geometry of the cluster. The dissociation times, decay rate constants, kinetic energy of the dissociating atoms and the geometrical structure of the remaining part of the clusters are computed from microcanonical sampling of the phase space. Distributions of these properties as well as the possibilities of various fragmentation channels are presented.

Introduction

Carbon clusters have been the focus of a great number of experimental and theoretical studies[1-3]. The basic driving force beneath all these efforts lies at the unusually high stability of large carbon clusters. However the structural and dynamical properties of small clusters are also of great interest. There are many questions related to the ground state conformations, relative stability of isomers and fragmentation-dissociation dynamics. The experimental studies[4-8] are mainly concentrated on ionic structures whereas the bulk of the theoretical efforts are on neutral clusters because of the computational problems of the electronic calculations for ionic systems.

The quantum mechanical calculations of various sophistication ranging from semiempirical or density functional approaches to large basis SCF+ configuration interaction schemes have been carried out for the structural stability of carbon clusters[9-15]. On the other hand, the dynamical structure cannot be studied by quantum mechanical approaches presently due to the high mathematical complexity of the problem. In that case, one usually resorts to mixed-mode methodologies combining quantum and classical philosophies or simply treat the system classically. Even though the classical methods ignore several important quantum effects such as tunneling or zero-point energy, they are algorithmically very practical allowing a reasonable sampling of the phase space. The basis of these approaches rely on the expansion of the interaction potential in terms of many-body interaction terms which can be then reduced into effective two-and three-body interactions with the help of the experimental data.

* This work is presented at 35th IUPAC-İstanbul Congress as an invited lecture.

The simplest approach to the development of the potential function for carbon clusters is a combination of the Lennard-Jones and Axilrod-Teller terms by fitting the weight of the three-body term so that it will give the relative stability of various isomers[16]. The more sophisticated potential functions are obtained by optimizing both the form and the parameters of functions so that many bulk properties are reproduced of different carbon structures such as diamond crystal or basal planes of graphite[17–18]. Another potential function with a somewhat longer range character is developed by Takai et. al. (TLHT) with the intention of reproducing both the bulk and the small cluster properties[19]. In our studies we employ this potential function which is composed of two- and three-body functions of the form:

$$U_r(r_i, r_j) = \exp(q_1 - q_2 r_{ij}) - q_3(1/2 - 1/\pi \tan^{-1}(q_4(r_{ij} - q_5)))^{12} \tag{1}$$

$$U_3(r_i, r_j, r_k) = Z(p + (\cos\Theta_i + h)(\cos\Theta_j + h)(\cos\Theta_k + h)) \exp(-b^2(r_{ij}^2 + r_{ik}^2 + r_{jk}^2)) \tag{2}$$

With the above functional form and 9 parameters, the ground state structures, binding energies and vibrational frequencies are computed for C_3, C_4 and C_5. The results agree with the experimental data much better then the other potential functions.

In this work, the dissociation dynamics of $C_n (2 < n < 7)$ are presented utilizing TLHT potential for the classical trajectory calculations.

Computational Aspects

The dynamical analysis is carried out by solving the Hamilton's equations using a 4th order Runge-Kutta algorithm with constant time-steps. Depending on the size of the cluster and energy, integrations are carried out up to 12 ps with the time step of 0.05 fs. Within this scheme the energy remains constant with the error of 10^{-6} eV. The sampling consists of 2000 trajectories at each energy and the geometry for C_3 and for larger clusters the averages are computed over 100 trajectories. The initial geometry are chosen as the equilibrium ones for each isomer and the momenta is distributed randomly to each atom. In Table 1 we present the binding energies of these structures in order to give an idea of the energy ranges studied within this work.

Table 1. Energies of carbon clusters from TLHT potential.

Cluster	Structure	Energy (eV)
C_3	Linear	-12.82
	Equilateral triangle	-12.56
C_4	Linear	-19.44
	Rhombus	-18.51
	Triangular Pyramidal	-16.39
C_5	Linear	-26.06
	Pentagonal	-25.68
	Tetrahedral	-22.23
C_6	Hexagonal	-33.66
	Linear	-32.68

For the rotating clusters the individual momentum components are scaled to the desired energy such that the total linear momentum is zero. For the nonrotating clusters, a Monte Carlo type minimization is

used to obtain zero angular momentum. Upon detecting a dissociating atom, the integration is stopped and various properties are computed.

C_3

We studied the dynamics of C_3 for the energy range -4.0 eV $< E < -0.2$ eV with increments of 0.2 eV. the initial geometry is changed from linear one to the equilateral triangle with 30° increments. In each case 2000 initial configurations are chosen as described above. Both the rotating and nonrotating clusters are treated separately to isolate the effects of the rotation of the clusters. Within 0.1 ps all the nonrotating clusters dissociated irrespective of the initial geometry. However the rotating clusters display a strong dependence on the initial geometry of the cluster. In Figure 1 this dependence is shown with corresponding energy of each cluster. The number of dissociating trajectories increase when the initial structure changes from the linear to equilateral triangle. Since all the kinetic energy is in the vibrational motion for the nonrotating clusters, it is easy to understand their relatively faster dissociation, but the initial geometry dependence for the rotating clusters suggest a somewhat complicated mechanism for the dissociation

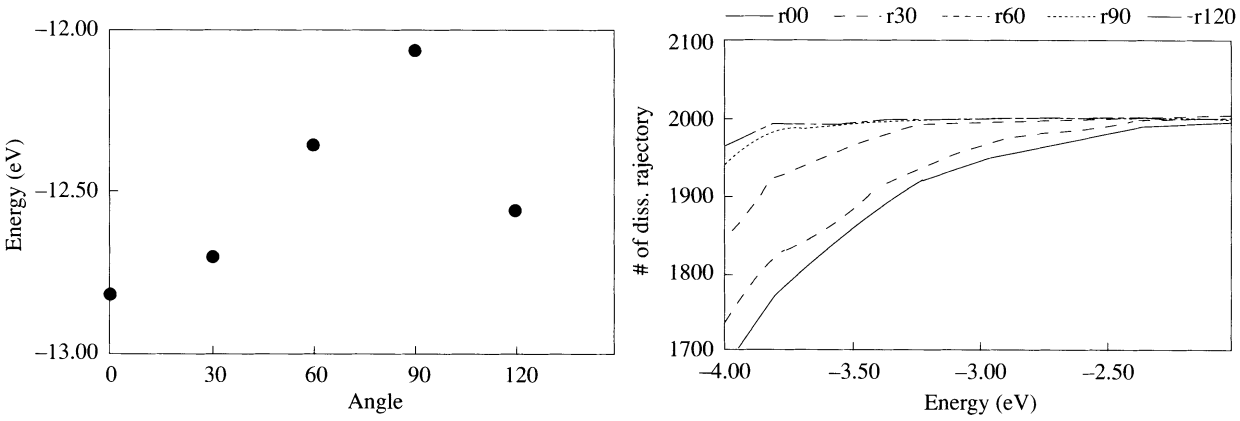

Figure 1. a) Energy of C_3 isomers, b) # of dissociating trajectories

When a dissociation is detected, the total momentum of the dissociating particle, the bond length of the remaining C_2 and the angle between the direction of the dissociating atom and C_2 are measured and averaged at each energy and the initial geometry for the rotating and nonrotating clusters separately.

In Fig. 2-4 these average values are presented as functions of the cluster energy. As it is expected from previous figures, the dissociation is faster for the nonrotating ones and the geometry dependence is not detected. The variation of the momentum and the length of the dimer follows the same trend.

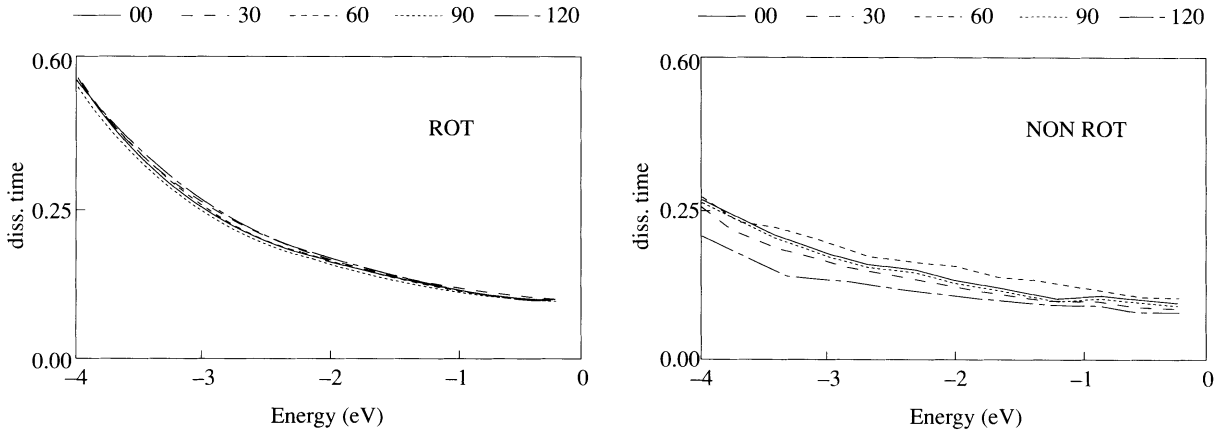

Figure 2. Average dissociation times for rotating and nonrotating clusters.

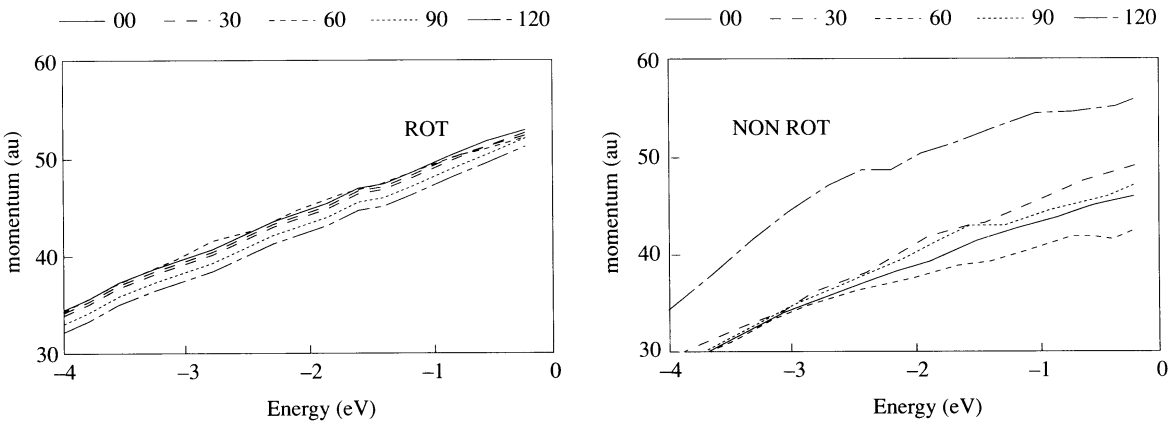

Figure 3. Average momentum of the dissociating atom for rotating and nonrotating clusters.

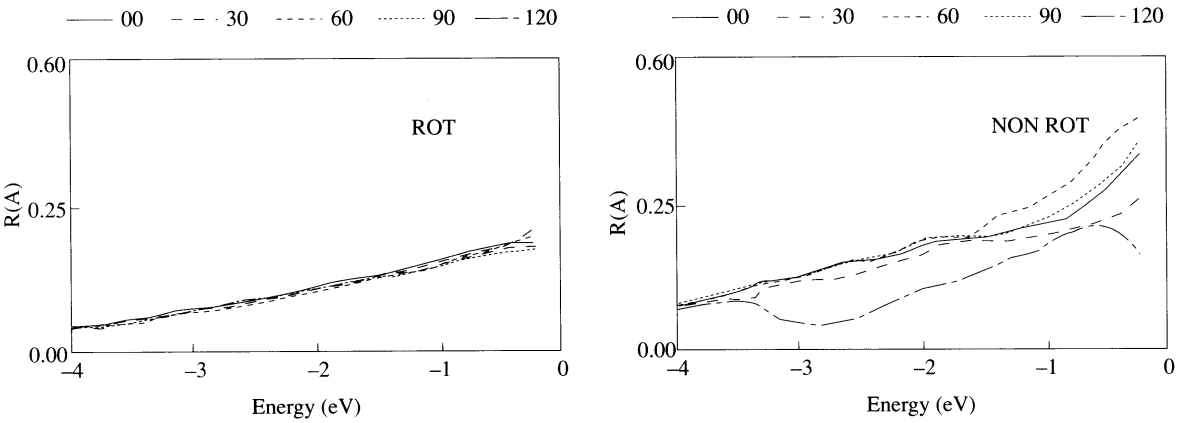

Figure 4. Average length of the remaining C_2 for rotating and nonrotating clusters.

One possible explanation for the above behaviour comes from the partitioning of the kinetic energy into vibrational and rotational ones. For the constant total energy, if there is no rotational motion, then the vibrational modes will have relatively larger temperatures causing faster dissociation. However the lifetime vs. total angular momentum plots completely deny any correlation between the rotational (or conversely vibrational) temperatures and dissociation times. At Fig. 5 we display the distribution of dissociation times at various energy values for the linear C_3. A large number of the trajectories dissociate within a small interval of 0.15 ps. As the total energy decreases, distributions become wider with no significant difference between the rotating and nonrotating clusters. In contrast the distribution of the directional angle of the dissociating atom show a strong correlation for the rotating clusters. Therefore we would like to conclude that the dissociation of C_3 clusters depend on the rotational motion in an indirect mechanism.

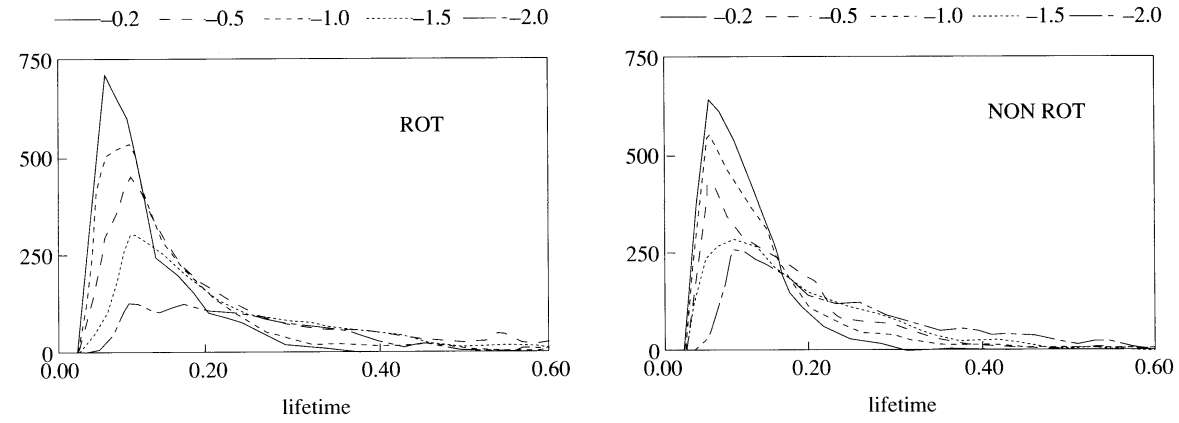

Figure 5. Distribution of lifetimes

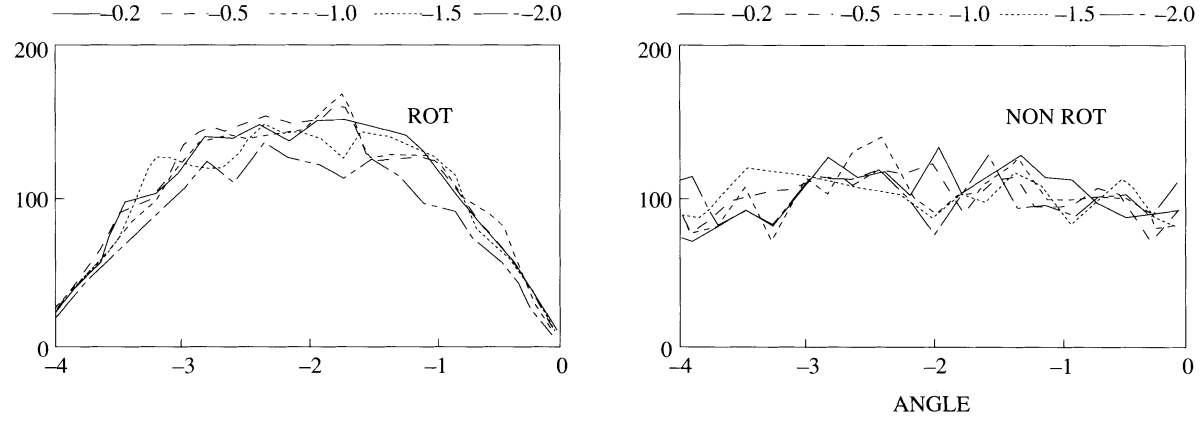

Figure 6. Distribution of directional angles of the dissociating atom.

C_4 - C_5 - C_6

For these clusters we have considered three shapes representing one, two and three dimensional structures. The energy ranges are chosen such that first and second dissociation channels can be detected. In each geometry and energy, 100 trajectory are used to sample the phase space with integration time of 12 ps. In Fig. 7 we present the average lifetimes of clusters of different shapes.

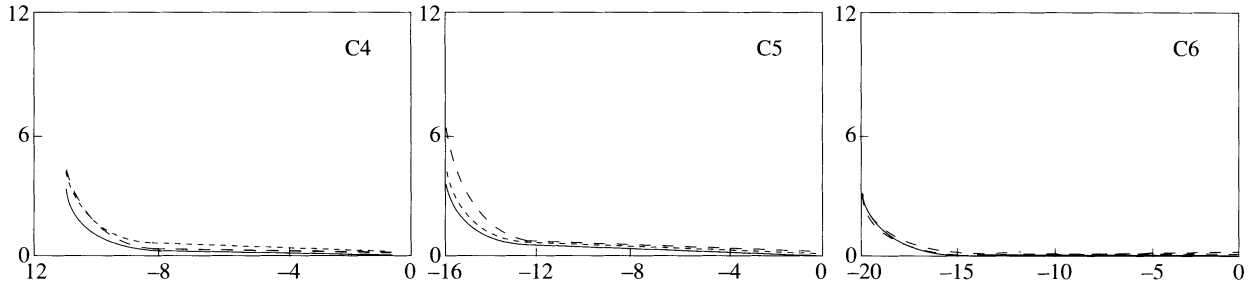

Figure 7. Average lifetimes for nonrotating C_n clusters.

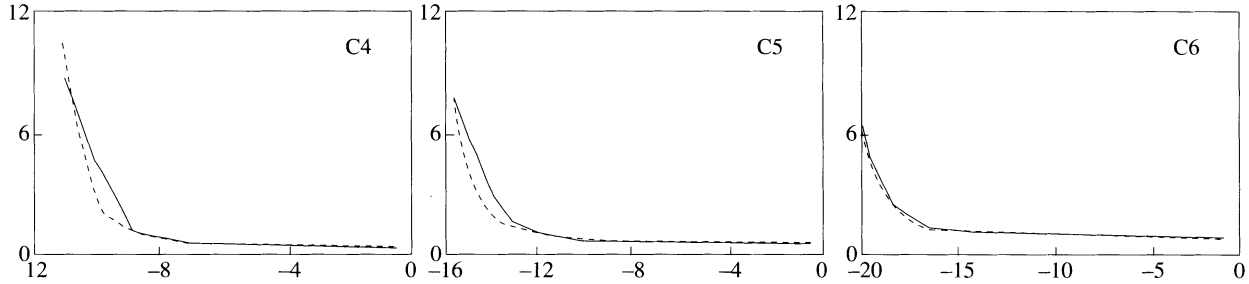

Figure 8. Average lifetimes for rotating C_n clusters.

Similar to our observations for C_3, the rotating clusters dissociate relatively slower and however the initial geometry does not play a significant role for these clusters.

The interesting problem for the dissociation of small clusters is the possibilities and time scales of various fragmentation channels. For the energy ranges considered, we observe the following channels:

1) $C_n \longrightarrow C_n$

2) $C_n \longrightarrow C_{n-1} + C$

3) $C_n \longrightarrow C_{n-2} + C_2$

4) $C_n \longrightarrow C_{n-2} + C + C$

5) $C_n \longrightarrow C_{n-1} + C \longrightarrow C_{n-2} + C + C$

It is relatively easy to distinguish these possibilities by monitoring clusters in the immediate vicinity of the first dissociation. In Fig. 9 we show the number of trajectories in each channel as functions of the total energy. For all clusters, the channels 2, 3 and 5 dominate the dynamics. For C_4 the more than half of the trajectories fail to dissociate the second carbon atom. When the second dissociation occurs, it is usually in the form of fragmenting into two dimers. However after the threshold energy of the channel 5 (energy of C_2 -6.2 eV) two successive dissociations with a relatively large time delay starts competing with this fragmentation. For C_5 and C_6 we observe different dynamical behaviour. At low energy regimes, again the loss of C_2 is the main channel for the second dissociation, but at higher energies the delayed dissociation of the second carbon atom becomes the most probable reaction.

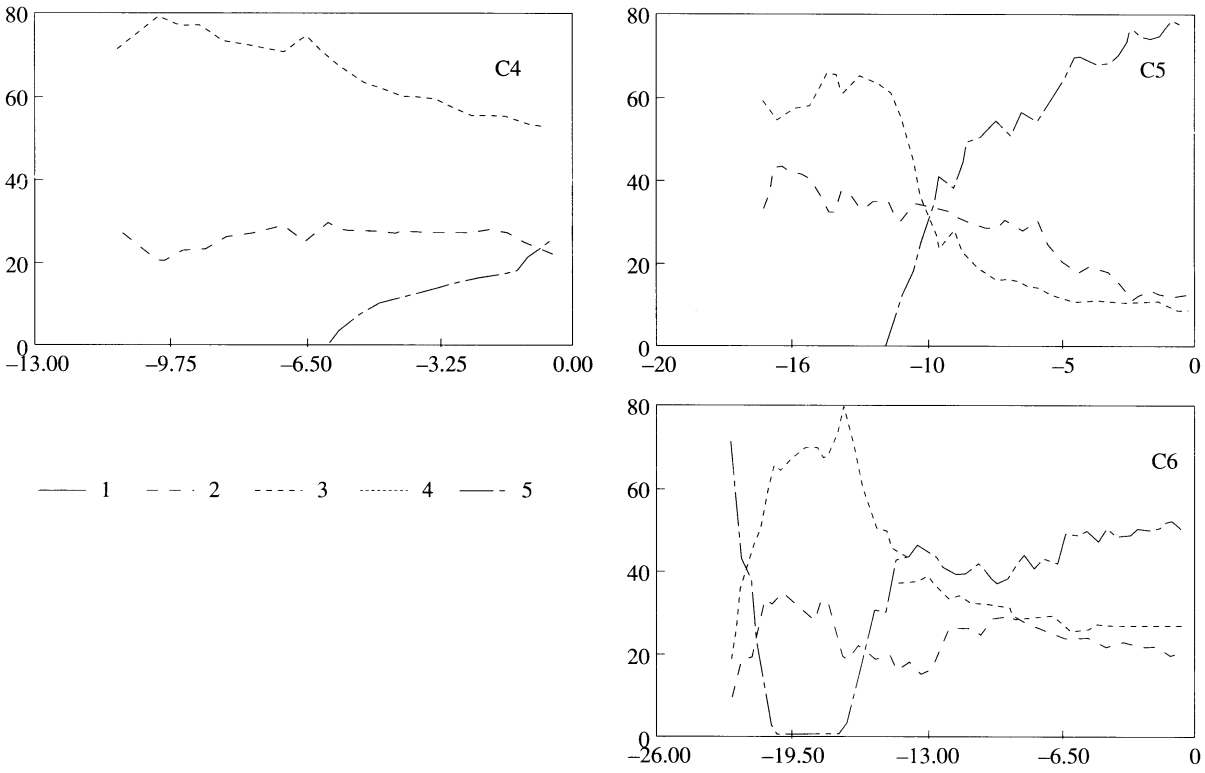

Figure 9. Dissociation probabilities

Conclusion

The dissociation dynamics of small carbon clusters show several interesting characteristics. The nonrotating clusters dissociate faster compared to nonrotating ones. For C_3 the initial geometrical structure also effects the dynamics strongly, but for larger clusters, this dependence is not observed. At low energies, the fragmentation resulting in $C_{n-2}+ C_2$ is the main channel whereas at higher energies successive dissociation of the second carbon atom with a time delay dominates the dynamics.

References

1. W. Weltner, Jr., R. J. Van Zee., **Chem. Rew., 89,** 1713 (1989).
2. S. Sugano, Micro Cluster Physics, Springer Series in Material Science, Springer-Verlag, Berlin, 87, (1991).

3. E.E.B. Campbell, Clusters of Atoms and Molecules, Springer Series in Chemical Physics, Springer-Verlag, Berlin, 331, (1995).
4. M. E. Geusic, T.J. Mcllrath, M.F. Jarrold, L.A. Bloomfield, R.R. Freeman, W.L. Brown, **J. Chem. Phys., 84,** 4421, 1986.
5. M.E. Geusic, M.F. Jarrold, T.J. Mcllrath, R.R. Freeman, W.L. Brown, **J. Chem. Phys., 86,** 3862, (1987).
6. S. Yang, K.J.: Taylor, M.J. Craycraft, J. Conceicao, C.L.: Pettiette, O. Cheshnovsky, R.S. Smalley, **Chem. Phys. Letters, 144,** 431, (1988).
7. A.N. Pargelis, **J. Chem. Phys., 93,** 2099, (1990).
8. S.W. McElvany, Int. J. Mass, **Spect. and Ion Process, 102,** 81, (1990).
9. B.K. Rao, S.N. Khanna, P. Jena, **Solid State Comm., 58,** 53 (1986).
10. D. Zajfman, D. Kella, O. Heber, D. Majer, H. Feldman, Z. Vager, R. Naaman, **Z. Phys. D 26,** 343 (1993).
11. R. Bleil, F.M. Tao, S. Kais, **Chem. Phys. Letters., 229,** 491, (1996).
12. M. Mladenovic, S. Schmatz, P. Botschwina, **J. Chem. Phys., 101,** 5891, (1994).
13. J. Hutter, H.P. Lüthi, **J. Chem. Phys., 101,** 2213, (1994).
14. W. Andreoni, D. Scharf, **Chem. Phys. Letters, 173,** 449, (1990).
15. E. Yurtsever, N. Elmacı, **Ber. Buns. Phys. Chem., 95,** 467, (1991).
16. J. Tersoff, **Phys. Rev. Letters, 61,** 2879 (1988).
17. D. J. Brenner, **Mater. Res. Soc., Symp. Proc., 141,** 59, (1989).
18. T. Halıcıoğlu, **Chem. Phys. Letters, 179,** 159, (1991).